


# A new frequency domain method for random fatigue life estimation in a wide-band stationary Gaussian random process

Qinghua Han<sup>1</sup> | Jia Li<sup>1</sup> | Jie Xu<sup>1</sup>  | Fei Ye<sup>1</sup> | Alberto Carpinteri<sup>2</sup> | Giuseppe Lacidogna<sup>2</sup>

<sup>1</sup>School of Civil Engineering, Tianjin University, Tianjin, China

<sup>2</sup>Department of Structural, Geotechnical and Building Construction, Politecnico di Torino, Italy

## Correspondence

Jie Xu, School of Civil Engineering, Tianjin University, Tianjin, China.  
Email: jxu@tju.edu.cn

## Funding information

Natural Science Foundation of Tianjin City, Grant/Award Number: 16JCQNJC07400; National Key Research and Development Plan of China, Grant/Award Number: 2016YFC0701103; National Natural Science Foundation of China, Grant/Award Number: 51525803

## Abstract

A new frequency domain method for random fatigue life estimation in a wide-band stationary Gaussian random process was proposed for application in fatigue analysis. Simulations of the power spectral densities of different types were firstly performed; the simulated results showed that the accuracy and applicability for the current frequency domain methods are not only related to the spectral type but also associated with the types of the analysed materials. Compared with the current methods, the proposed method, in which the rain-flow amplitude obeys Nakagami distribution, has better universality and could significantly reduce the error for the random fatigue life estimation with simulated and actual spectra. Verified application in cast-steel fatigue life analysis were performed between random fatigue life and constant amplitude fatigue life. It is shown that the fatigue life analysis under random load cannot be ignored and the proposed new method can serve as a recommended method.

## KEYWORDS

frequency domain method, life estimation, power spectral density, probability density function, random load, time domain

## 1 | INTRODUCTION

With the rapid development of modern structures, the socio-economic losses caused by the failure of engineering structures have been increasing in recent years. Fatigue, as one of the main failure modes with strong sudden and severe destruction, is a widespread problem in various fields of civil engineering and other fields.

For example, the American Kings steel bridge collapsed via fatigue in 1962, causing heavy economic losses.<sup>1</sup> The semi-submersible platform Alexan-derkeyland sank in the North Sea<sup>2</sup> in 1980, primarily because of structural fatigue. A Boeing 747-209b of a Chinese airline crashed into the sea at 35 000 feet off the coast of Penghu because of metal fatigue in 2002. Based on the above cases, fatigue has always been an issue.

**Nomenclature:**  $C$ ,  $k$ , = material parameter;  $D$ , = fatigue damage;  $M$ , = shape parameter;  $m_i$ , = the  $i$ th spectral moment;  $p(s)$ , = cycle amplitude probability density function;  $S$ , = stress amplitude;  $\sigma^2$ , = the mean square value of the random process.;  $RE$ , = relative error;  $T$ , = fatigue life;  $s_a$ , = the rain-flow stress amplitude;  $s_m$ , = the rain-flow mean stress;  $s_u$ , = tensile strength;  $X_k$ , = spectral values;  $x_m$ , = the simulated time domain signal;  $\alpha_i$ , = spectral width parameter;  $\nu_0$ , = expected positive zero-crossing rate;  $\nu_p$ , = expected peak occurrence frequency;  $\Omega$ , = scale parameter;  $\mu$ , = location parameter;  $\nu$ , = shape parameter; RF, = rain flow-counting method; NB, = narrow-band method; WL, =Wirsching-Light method; AL, =  $\alpha_{0.75}$  method; OC, = Ortiz and Chen method; TB1, = Tovo-Benasciutti method 1; TB2, = Tovo-Benasciutti method 2; DI, = Dirlik method; ZB, = Zhao-Baker method; SM, = single-moment method

Fatigue research is often based on constant fatigue and variable amplitude fatigue; however, in fact, random fatigue loads due to environment, equipment, pedestrians, vehicles, and other factors widely exist and are inevitable. The traditional method to estimate the random life is to multiply the constant amplitude load by an amplification factor to consider the random load; however, this approach will lead to some problems, such as the overall fatigue strength of the frame being too high and that of the local structure being inadequate, and it is not consistent with the actual situation. Thus, the analysis of the fatigue characteristics under random loads has significant research value.

In the earlier research, random fatigue life estimation involves time domain and frequency domain methods. The time domain method studies the response stress time history, and the key is the cycle counting of the equivalent stress ranges based on the time series that can be obtained experimentally or numerically.<sup>3</sup> Based on this theory, many scholars have proposed different cycle-counting methods, such as peak counting, level-crossing counting, range counting, and rain-flow counting. Among them, the rain flow-counting method is considered to be the most accurate fatigue damage estimation method<sup>4-7</sup>; this method is commonly applied as a reference to check the accuracy of frequency domain methods. However, the time-history determination or simulation represents a more expensive and time-consuming part of the overall work. To reduce the uncertainty of the results and obtain a stable fatigue damage estimation, a large number of time series samples with long enough durations must be simulated; this process is not feasible in engineering applications. Thus, other approaches (such as the frequency domain method) that reduce the time required for stress evaluation are clearly welcome.

The frequency domain method is developed on the basis of the time domain method and has obvious advantages over the time domain method. The frequency domain method mainly uses statistics on the frequency domain for fatigue life estimation and avoids consideration of a randomly varying time history, thereby greatly simplifying the calculation process and improving the operating speed. Associated with material  $S-N$  curves and an appropriate damage theory,<sup>8</sup> the frequency domain method mainly does research about the power spectral density (PSD) in the frequency domain and estimates the random fatigue life through its various statistical characteristic values. In application of the frequency domain method, the critical step is to obtain the probability density distribution function of the stress amplitude. For a narrow-band random process, Bendat and Piersol<sup>9,10</sup> proposed that the probability density function

(PDF) of its rain-flow amplitude obeys a Rayleigh distribution, as confirmed by theory. For a wide-band random process, there are still no theoretical functions able to accurately describe the PDF. However, many empirical formulas of the PDF have been derived by experiment and simulation, such as the Wirsching-Light method,<sup>11</sup> the G. Chaudhury method,<sup>12</sup> the Jiao and Moan method,<sup>13</sup> the Benasciutti-Tovo method,<sup>14</sup> the Dirlik method,<sup>15,16</sup> and the Zhao-Baker method.<sup>17</sup>

In this paper, the primary study of the stochastic fatigue questions is performed. Because of the superiority of the frequency domain method compared with the time domain method, this paper mainly focuses on the random lifetime prediction in the frequency domain. First, a brief review of several common frequency domain methods is provided; these methods are compared for different materials and for different simulated PSDs. Next, to identify a frequency domain method with better applicability and higher accuracy, a new fatigue life estimation model considering the mean stress is presented, and a relationship between fatigue damage and the statistical parameters of the PSD is established. A new formula of the frequency domain method is proposed. Finally, a simple application is performed to verify the applicability of the new method. The calculation results of the application are compared with the fatigue life under the constant amplitude load in the reference, which shows the negative influence of the random load.

## 2 | BRIEF REVIEW AND COMPARISON OF THE CURRENT FREQUENCY DOMAIN METHODS

### 2.1 | Brief review of the current frequency domain methods

Typical methods to consider stationary Gaussian random loads for fatigue analysis in the frequency domain are discussed in detail in our previous paper<sup>18</sup>; a concise review of these methods is provided here for better understanding of the following section.

Generally, random vibration load can be assumed as a stationary Gaussian stochastic process  $X(t)$ . In the frequency domain, the random process  $X(t)$  is defined by the PSD  $S_{xx}(f)$ , which is a bilateral symmetrical spectrum. A 1-sided PSD  $G_{xx}(f)$  can be used as a research object instead of the bilateral symmetrical spectrum, which is defined on the positive half axis only. For a stationary Gaussian random process, the statistical properties can be described by the spectral moments of the  $G_{xx}(f)$ . The general form for the  $i$ th spectral moment  $m_i$  is given by

$$m_i = \int_0^\infty f^i G_{xx}(f) df. \quad (1)$$

The unit of frequency  $f$  is Hz. In particular, the variance of random process  $X(t)$  can be represented as  $\sigma_x^2 = m_0$ , and the spectral width parameter can be expressed as follows:

$$\alpha_i = \frac{m_i}{\sqrt{m_0 m_{2i}}}. \quad (2)$$

The most popularly used  $\alpha_2$  is called the irregular factor, varying between 0 and 1, which is defined to distinguish the bandwidth characteristics of the stochastic process  $X(t)$ . The random process  $X(t)$  tends to be white noise when  $\alpha_2 \rightarrow 0$ , and it tends to be a narrow-band random process when  $\alpha_2 \rightarrow 1$ .

In the frequency domain method, the expected peak occurrence frequency  $\nu_p$  and the expected positive zero-crossing rate  $\nu_0$  are 2 important parameters defined as

$$\nu_p = \sqrt{\frac{m_4}{m_2}}, \nu_0 = \sqrt{\frac{m_2}{m_0}}. \quad (3)$$

To calculate the random fatigue life of the structure, the frequency domain method focuses on the fatigue damage per unit of time. Generally, the material  $S$ - $N$  curve is in the following form:

$$N \cdot s^k = C. \quad (4)$$

Combined with the linear Miner cumulative damage theory, the fatigue damage per unit of time can be expressed as

$$D = \nu_p C^{-1} \int_0^\infty s^k p(s) ds, \quad (5)$$

where  $\nu_p$  is the expected peak occurrence frequency given by Equation 3.  $C$  and  $k$  are material parameters shown in Equation 4, and  $p(s)$  is the rain-flow amplitude PDF. The determination of function  $p(s)$  is the key factor in the frequency domain method for fatigue analysis.

Fatigue failure occurs when  $D \cdot T$  reaches 1; thus, the random fatigue life of the structure is defined by

$$T = \frac{1}{D}. \quad (6)$$

The methods described here are relevant for the wide-band stationary Gaussian random process, whose spectral density curve takes meaningful values over a wide frequency band and whose statistical properties include time and random variables that obey a Gaussian distribution; the methods follow the general procedure for fatigue analysis in the frequency domain.

## 1) Narrow-band method (NB)

For the narrow-band random process, Bendat proposed that the rain-flow amplitude of each cycle is completely symmetrical; thus, the PDF tends to obey Rayleigh distribution.  $\nu_0$  is very close to the peak intensity  $\nu_p$  for a narrow-band process<sup>19</sup>; thus,  $\nu_p$  in Equation 5 will be replaced by  $\nu_0$  here. The PDF and damage per unit of time estimation formula are defined as follows:

$$p(S) = \frac{S}{\sigma^2} \exp\left(-\frac{S^2}{2\sigma^2}\right), \quad (7)$$

$$D^{NB} = \nu_0 \int_0^\infty \frac{p(S)}{f(S)} dS, \quad (8)$$

where  $f(S)$  denotes  $N$  in the material  $S$ - $N$  curve that can be derived from Equation 4.

## 2) Wirsching-Light method (WL)

Wirsching and Light corrected the narrow-band method with the empirical coefficient  $\rho_{WL}$  in 1980.

$$D^{WL} = \rho_{WL} D^{NB}, \quad (9)$$

where  $\rho_{WL} = a(k) + [1 - a(k)](1 - \varepsilon)^{b(k)}$ , with the spectral width parameter  $\varepsilon = \sqrt{1 - \alpha_2^2}$ , and the best fitting parameters  $a$  and  $b$  are dependent on the slope  $k$  of the  $S$ - $N$  curve:

$$\begin{aligned} a(k) &= 0.926 - 0.033k, \\ b(k) &= 1.587k - 2.323. \end{aligned} \quad (10)$$

## 3) $\alpha_{0.75}$ method (AL)

As expressed in Equation 11, Benasciutti and Tovo proposed a new spectral width parameter  $\alpha_{0.75}$  from numerical simulation data, which is used as a modified factor to correct the narrow-band method.

$$D^{AL} = \alpha_{0.75}^2 D^{NB} \quad (11)$$

## 4) Ortiz and Chen method (OC)

Ortiz and Chen developed the following correction factor by applying the generalized spectral bandwidth to the Rayleigh distribution<sup>20,21</sup>:

$$D^{OC} = \zeta_k D^{NB}, \quad (12)$$

$$\zeta_k = \frac{1}{\alpha_2} \left( \sqrt{\frac{m_2 m_k}{m_0 m_{k+2}}} \right)^k, \quad (13)$$

for which  $k' = 2.0/k$ .

### 5) Tovo-Benasciutti method

Tovo and Benasciutti found that the rain-flow damage of the Gaussian process  $D_{RFC}$  is between the Rayleigh fatigue damage  $D_{NB}$  and the range counting damage  $D_{RC}$ :

$$D_{RC} \leq D_{RFC} \leq D_{NB}. \quad (14)$$

Thus, the rain-flow damage can be written as

$$D_{BT} = bD_{NB} + (1-b)D_{RC},$$

where  $D_{RC} \cong D_{NB}\alpha_2^{k-1}$ ; thus,

$$D^{TB} = [b + (1-b)\alpha_2^{k-1}]\alpha_2 D^{NB}. \quad (15)$$

Two different equations are suggested for determining the factor  $b$ :

$$b^{TB1} = \min\left\{\frac{\alpha_1 - \alpha_2}{1 - \alpha_1}, 1\right\}, \quad (16)$$

$$b^{TB2} = \frac{(\alpha_1 - \alpha_2)[1.112(1 + \alpha_1\alpha_2 - (\alpha_1 + \alpha_2))e^{2.11\alpha_2} + (\alpha_1 - \alpha_2)]}{(\alpha_2 - 1)^2}. \quad (17)$$

According to the value of  $b$  in Equations 16 and 17, the method is called TB1 and TB2, respectively.

### 6) Dirlik method (DI)

The Dirlik method is a closed empirical formula derived from a large number of experiments and numerical simulations and has been considered to be the most widely used method for a long time. The Dirlik method uses a combination of 1 exponential distribution and 2 Rayleigh distributions to approximate the rain-flow amplitude probability density distribution.

$$p(Z) = \frac{D_1}{Q} e^{\frac{-Z}{Q}} + \frac{D_2 Z}{R^2} e^{\frac{-Z^2}{2R^2}} + D_3 Z e^{\frac{-Z^2}{2}} \quad (18)$$

where

$$D_1 = \frac{2(\chi_m - \gamma^2)}{1 + \gamma^2}, \quad D_2 = \frac{1 - \gamma - D_1 + D_1^2}{1 - R},$$

$$D_3 = 1 - D_1 - D_2, \quad Z = \frac{S}{\sqrt{m_0}}, \quad \gamma = \frac{m_2}{\sqrt{m_0 m_4}},$$

$$Q = \frac{1.25(\gamma - D_3 - D_2 R)}{D_1}, \quad R = \frac{\gamma - \chi_m - D_1^2}{1 - \gamma - D_1 + D_1^2}, \quad \chi_m = \frac{m_1}{m_0} \sqrt{\frac{m_2}{m_4}}.$$

### 7) Zhao-Baker method (ZB)

This fatigue model gives an expression for the cycle distribution as a linear combination of the Weibull and Rayleigh PDFs.

$$p(Z) = \eta ab Z^{b-1} e^{-aZ^b} + (1-\eta) Z e^{-\frac{Z^2}{2}}, \quad (19)$$

where the parameters are expressed as

$$a = 8 - 7\alpha_2,$$

$$\eta = \frac{1 - \alpha_2}{1 - \sqrt{\frac{2}{\pi}} \Gamma\left(1 + \frac{1}{b}\right) a^{-1/b}} b = \begin{cases} 1.1 & \alpha_2 < 0.9 \\ 1.1 + 9(\alpha_2 - 0.9) & \alpha_2 \geq 0.9 \end{cases}.$$

### 8) Single-moment method (SM)

The Larsen and Lutes' single moment method<sup>22,23</sup> was developed after extensive examination of the simulation data and rain-flow analysis, particularly for bimodal PSDs:

$$D^{SM} = \zeta_{SM} D^{NB}, \quad (20)$$

$$\zeta_{SM} = \frac{(m_k'/m_0)^{k/2}}{v_0}. \quad (21)$$

## 2.2 | Comparison of the methods

The accuracy of a good frequency domain method is not only suitable to the spectral type but also applicable for different types of material. Therefore, a comparison through the numerical simulations with different simulated spectra and 3 different materials will be performed to check the accuracy and applicability of the aforementioned methods.

### 2.2.1 | Simulated spectra

Simulated spectra can be divided into the following 4 categories: unimodal spectra, bimodal spectra, multimode spectra, and white noise spectra. In addition, 3 typical engineering spectra based on real data were selected to ensure the reliability of the results.

#### 1) Unimodal spectra

Unimodal spectra refer to the PSD that has only 1 peak in the entire curve. As shown in Figure 1, there are a total of 5 simulated curves in this group, which are positioned at the central frequencies  $f_c$  of 50, 100, and 150 Hz, with wave width  $b$  values of 5, 10, and 15 Hz as well as stress PSD amplitudes of 500, 1000, 1500, and 2300  $\text{Mpa}^2/\text{Hz}$ .

#### 2) Bimodal spectra

Bimodal spectra characterized by only 2 main frequency peaks in the whole process represent one of

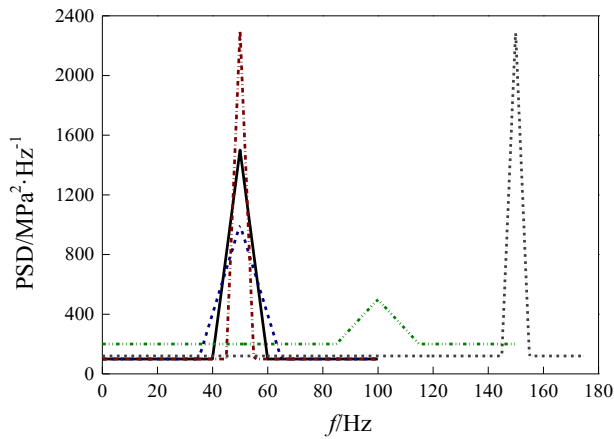


**FIGURE 1** Unimodal spectra. PSD, power spectral density [Colour figure can be viewed at [wileyonlinelibrary.com](http://wileyonlinelibrary.com)]

the basic forms of the engineering structural dynamic response. Figure 2A contains 3 curves, and the 2 peaks in each curve are completely independent. In Figure 2B, the 2 peaks of the bimodal spectra approach each other and have different degrees of overlap. In addition, the bimodal centre frequency  $f_c$ , peak width  $b$ , and the amplitude also take different combinations in each curve.

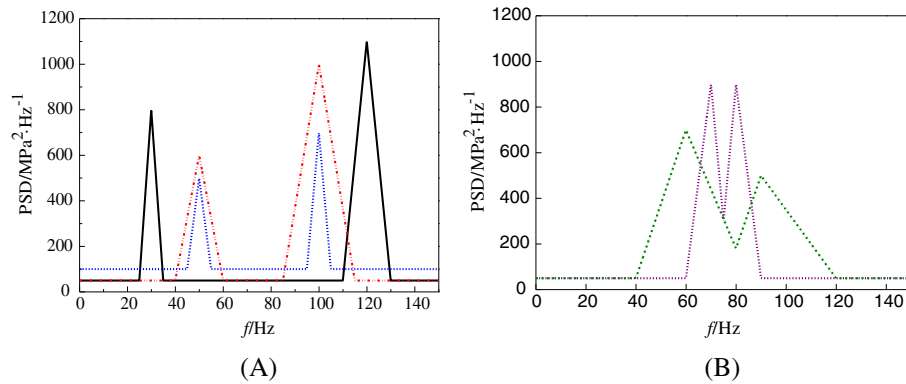


**FIGURE 2** Bimodal spectra. PSD, power spectral density [Colour figure can be viewed at [wileyonlinelibrary.com](http://wileyonlinelibrary.com)]

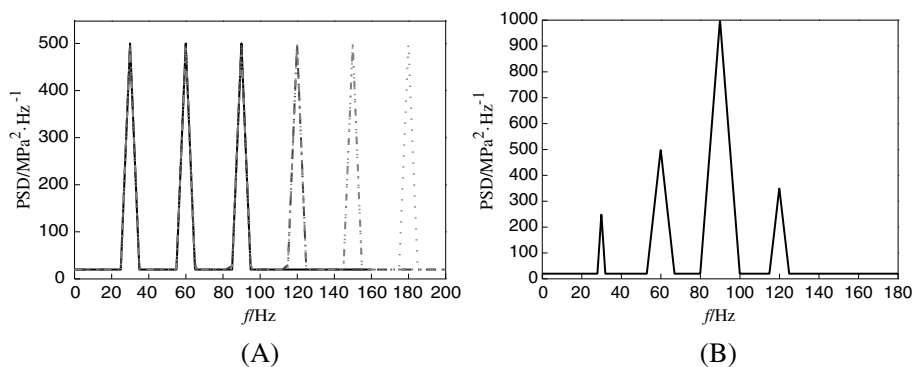


**FIGURE 3** Multimode spectra. PSD, power spectral density [Colour figure can be viewed at [wileyonlinelibrary.com](http://wileyonlinelibrary.com)]

### 3) Multimode spectra

Multimode spectra commonly exist in civil structures, mechanical and marine engineering, having 3 or more peaks over the entire frequency range. Figure 3A includes 4 curves, with the first one having only 3 peaks, and each subsequent curve having 1 additional mode (up to a maximum 6). The modes are positioned at the central frequencies  $f_c$  of 30, 60, 90, and 120 Hz with amplitudes of 500 MPa<sup>2</sup>/Hz. Figure 3B contains a spectrum curve with 4 peaks, of which the peak width and peak value are not the same to exclude the exceptional case of the simulated spectra.

### 4) White noise

White noise is a typical form of wide-band spectra, whose spectral density acts as a uniform straight line with unlimited bandwidth. In fact, this spectrum does not exist in nature; nevertheless, the smooth signals with limited bandwidth can be treated as white noise in engineering. In this group, 3 white noise spectra with the same amplitude were simulated, as shown in Figure 4A, and the central frequencies lie at 60, 60, and 120 Hz, with bandwidths of 20, 30, and 20 Hz, respectively. With the background noise increasing from 0 to 100 MPa<sup>2</sup>/Hz, Figure 4B

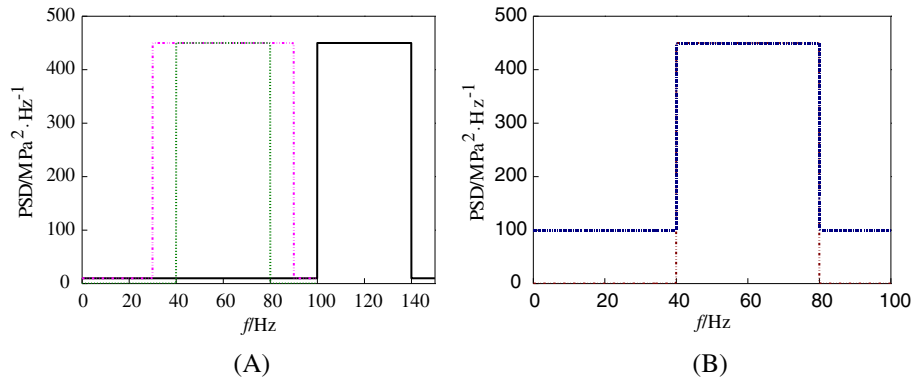


**FIGURE 4** White noise spectra. PSD, power spectral density [Colour figure can be viewed at [wileyonlinelibrary.com](http://wileyonlinelibrary.com)]

considers the effect of the background noise on the estimation accuracy of the frequency domain methods.

##### 5) Typical engineering spectra

To test the applicability of various methods in real fatigue loads, 3 realistic typical engineering spectra were selected in this study, as shown in Figure 5. The first curve<sup>24</sup> is a real engineering spectrum measured in the automotive industry. The second curve<sup>25</sup> is related to the stress process that occurs at the most stressed point of a bracket supporting a pressed circuit installed in a serial vehicle. The third curve<sup>26</sup> is obtained from a clamped-clamped beam simulation with damping ratio of 0.05 at 1/4 of the beam length.

## 2.2.2 | Applied materials

For the fatigue life calculation by using frequency domain methods, the  $S$ - $N$  curve of material also has an important influence. To ensure that the results have sufficient credibility, this article considers the 3 different materials

shown in Table 1. Among these materials, steel is the most widely used material in civil engineering. Aluminium is commonly used in the aerospace field and mechanical manufacturing field. Spring steel is used to make elastic elements. The  $S$ - $N$  curves use the power function form and the 3-parameter form, with the  $C$ ,  $k$  parameters and ultimate tensile strength changing significantly to cover the nearly the entire variation range of the relevant parameters in commonly used engineering materials. For the 3-parameter form  $S$ - $N$  curve, it is assumed that the load amplitude below material fatigue limit does not cause fatigue damage.

## 2.2.3 | Referenced criteria-time domain analysis

The fatigue life estimation results by using frequency domain method can be compared with the time domain. The rain-flow life  $T_{RF}$  is considered as an exact reference value among the different time domain methods.

Before using the rain flow-counting method, the PSD must be transferred from the frequency domain to the

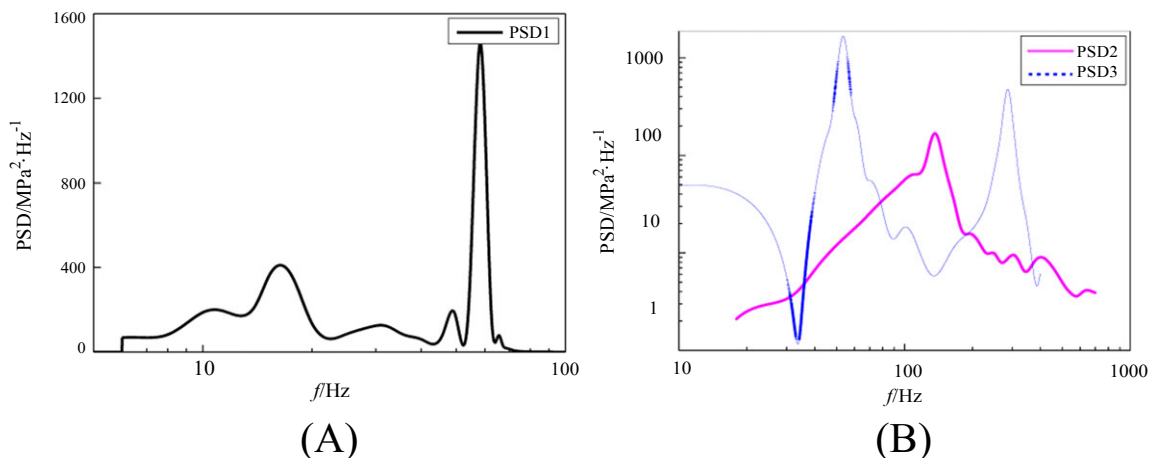


**FIGURE 5** Typical engineering spectra. PSD, power spectral density [Colour figure can be viewed at [wileyonlinelibrary.com](http://wileyonlinelibrary.com)]



**TABLE 1** Materiel parameters

	<b>S-N Curve</b>	<b>Su/MPa</b>
Steel	$N = 1.934 \times 10^{12} \times S^{-3.324}$	725
Aluminium	$N = 3.83 \times 10^{13} [S^{1.78} - 162.2^{1.78}]^{-2}$	425
Spring steel	$N = 1.413 \times 10^{37} \times S^{-11.7}$	1850

time domain. In this process, the amplitude and phase information of the signal is necessary. However, the simulated spectra only contain the amplitude information, ie, this process is unable to restore the time domain signal directly. For a stationary random process, it could be assumed that the random phase angle is uniformly distributed within the interval  $[0-2\pi]$ .<sup>27</sup> Thus, through reasonable assumptions, the time history with the same statistical properties of the original time domain signal can be obtained.

For each PSD, on the basis of the Nyquist theorem,  $f_s \geq 2f_{\max}$ , and the proper values of the sampling frequency  $f_s$  and the sampling points  $N$  must be set. Thus, the frequency range  $[0-f_{\max}]$  is dispersed to a number of discrete intervals with the length of  $\Delta f$  via sampling. According to the definition of the PSD, the relationship between PSD  $G_{xx}(k)$  and spectral values  $X_k$  can be represented as

$$|X_k| = \sqrt{\frac{N^2 \Delta f}{2}} G_{xx}(k). \quad (22)$$

The modulus of spectral amplitude  $|X_k|$  is given above, and the phase  $\varphi_k$  could be randomly selected in the interval  $[0-2\pi]$  because of the Gaussian stationary random process; thus, it can be written as

$$X_k = |X_k| e^{j\varphi_k}. \quad (23)$$

Discrete Fourier transform between the frequency domain and the time domain satisfies the following relationship. Combined with the Monte Carlo method, the simulated time domain signal  $x_m$  can be obtained.

$$X_k = \sum_{m=0}^{N-1} x_m e^{-j2\pi km/N} \quad (24)$$

By using the rain flow-counting method to obtain the simulated random time history, the rain-flow amplitude and mean stress can also be obtained. According to Kihl and Sarkani, the Goodman equation<sup>28-30</sup> can provide a reasonable and conservative prediction of the fatigue life, whether the mean stress is tensile or compressive. Therefore, the Goodman equation is applied to consider mean stress effects in this paper:

$$\frac{S_a}{S_{eq}} + \frac{S_m}{S_u} = 1. \quad (25)$$

Finally, the  $S$ - $N$  curve and the Miner cumulative damage rule are put into the rain-flow life estimation.

$$D_{RF} = \sum \frac{1}{N_i} = \sum \left( \frac{S_u \cdot (S_a)_i}{S_u - (S_m)_i} \right)^k / C \quad T_{RF} = \frac{1}{D_{RF}} \quad (26)$$

For comparison, because the phase angle information is simulated, the obtained time domain signal is also a random process. However, through statistics, it is found that, with the increases of sampling points  $N$  and the duration of time domain signal, the stability of fatigue life prediction will be improved. Therefore, this article took  $N$  as  $2^{17}$ , and 30 time domain samples for each PSD were simulated. Figure 6A,B represents the frequency and time domains, respectively, before and after the transformation. In Figure 6C, the simulated time domain signal of Figure 6B was transferred into the frequency domain in reverse for comparison with the original PSD in Figure 6A, showing that the two coincide with each other. Figure 7 is the statistical results of Figure 6B obtained by the rain-flow counting.

## 2.2.4 | Comparison results

The percentage of the life estimation relative error for each method is listed in Tables 2, 3, and 4, taking into account all the simulated spectra, where the relative error  $RE$  is calculated as

$$RE = \frac{|T_{RF} - T_{XX}|}{T_{RF}}. \quad (27)$$

$T_{XX}$  is the life estimation calculated according to Equations 7 to 21.

The results in Tables 2, 3, and 4 are based on the random fatigue life estimation results obtained by different frequency domain methods through 23 simulated spectra and the 3 types of materials mentioned above. For each material and for each frequency domain method, each simulated spectrum will obtain 1 fatigue life result and 1 relative error  $RE$  calculated by Equation 27. The percentage of results in table denotes the ratio of the number of simulated spectra under certain relative error  $RE$  to 23 total curves. For example, for the DI method, 0 indicates that the relative errors  $RE$  of all the simulated spectra are higher than 0.1.

From Tables 2, 3, and 4, we know that the applicability of the frequency domain methods to different materials are not the same. The frequency domain method for the applicability of the steel has, in general, the

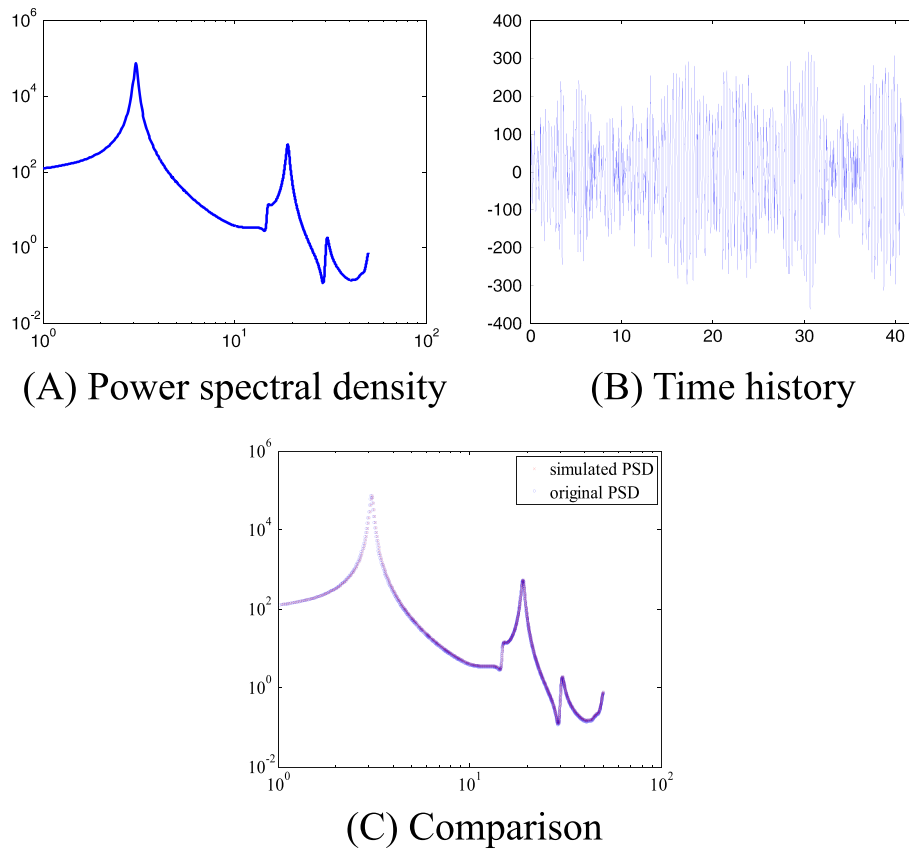


**FIGURE 6** Transformation of the time and frequency domains. A, Power spectral density; B, time history; and C, comparison. PSD, power spectral density [Colour figure can be viewed at [wileyonlinelibrary.com](http://wileyonlinelibrary.com)]

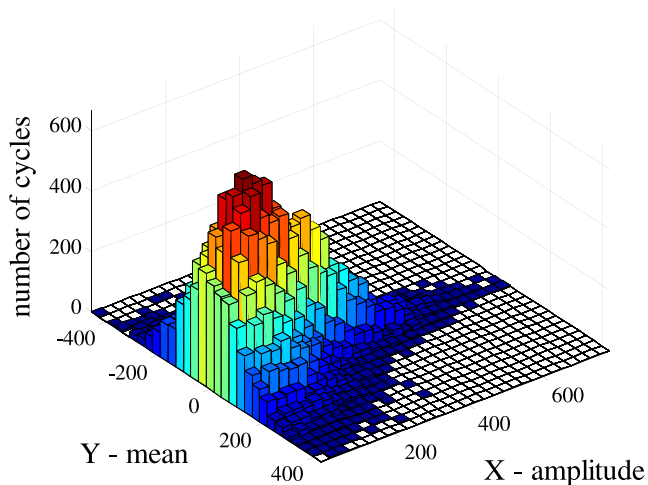


**FIGURE 7** Rain-flow counting [Colour figure can be viewed at [wileyonlinelibrary.com](http://wileyonlinelibrary.com)]

highest accuracy, followed by aluminium and spring steel, which are affected by the slope  $k$  of different  $S-N$  curves. For each material, the accuracy of different frequency domain methods is also different. For steel in Table 2, NB and TB1 have the maximum error, whereas TB2 and WL estimate results more accurately, with the

**TABLE 2** Percentage of relative errors for different margins for steel

	Rel. Error					
	<0.1	<0.2	<0.3	<0.4	<0.5	<0.6
NB	0	0	8.70	43.48	95.65	100.00
WL	4.35	13.04	56.52	95.65	100.00	100.00
AL	0	4.35	34.78	82.61	95.65	100.00
OC	0	4.35	26.09	82.61	95.65	100.00
TB1	0	0	13.04	47.83	95.65	100.00
TB2	8.70	47.82	91.30	95.65	100.00	100.00
DI	0	8.70	26.08	82.61	100.00	100.00
ZB	0	8.70	26.08	82.61	100.00	100.00
SM	0	4.35	43.48	86.96	95.65	100.00
% of results						

Abbreviations: AL,  $\alpha_{0.75}$  method; DI, Dirlik method; NB, narrow-band method; OC, Ortiz and Chen method; SM, single-moment method; TB1, Tovo-Benasciutti method 1; TB2, Tovo-Benasciutti method 2; WL, Wirsching-Light method; ZB, Zhao-Baker method.

error mainly in the range of 10% to 40% on the conservative side. For aluminium in Table 3, NB and TB1 lead to overly conservative estimation, whereas TB2 and DI are



**TABLE 3** Percentage of relative errors for different margins for aluminum

	Rel. Error					
	<0.1	<0.2	<0.3	<0.4	<0.5	<0.6
NB	0	0	0	13.04	78.26	91.30
WL	0	0	17.39	73.91	91.30	100.00
AL	0	0	8.70	56.52	86.96	91.30
OC	0	0	8.70	39.13	86.96	91.30
TB1	0	0	4.35	13.04	86.96	91.30
TB2	0	4.35	17.39	73.91	86.96	95.65
DI	4.35	8.70	13.04	82.61	86.96	100.00
ZB	0	0	8.70	47.83	86.96	95.65
SM	0	4.35	13.04	60.87	86.96	95.65
% of results						

Abbreviations: AL,  $\alpha_{0.75}$  method ; DI, Dirlik method; NB, narrow-band method; OC, Ortiz and Chen method; SM, single-moment method; TB1, Tovo-Benasciutti method 1; TB2, Tovo-Benasciutti method 2; WL, Wirsching-Light method; ZB, Zhao-Baker method.

**TABLE 4** Percentage of relative errors for different margins for spring steel

	Rel. Error					
	<0.1	<0.2	<0.3	<0.4	<0.5	<0.6
NB	0	0	0	0	13.04	34.78
WL	13.04	17.39	43.48	69.57	95.65	100.00
AL	0	0	0	8.70	17.39	56.52
OC	0	0	4.35	4.35	17.39	65.22
TB1	0	4.35	0	0	13.04	39.13
TB2	4.35	8.70	8.70	26.09	69.57	91.30
DI	0	4.35	4.35	13.04	21.74	69.57
ZB	0	0	0	4.35	17.39	52.17
SM	0	0	8.70	13.04	26.09	65.22
% of results						

Abbreviations: AL,  $\alpha_{0.75}$  method ; DI, Dirlik method; NB, narrow-band method; OC, Ortiz and Chen method; SM, single-moment method; TB1, Tovo-Benasciutti method 1; TB2, Tovo-Benasciutti method 2; WL, Wirsching-Light method; ZB, Zhao-Baker method.

better but also conservative, with 30% to 50% error. For spring steel in Table 4, neither of NB, AL, TB1, and ZB does well, whereas WL and TB2 are in good agreement; however, the error is still above 40%.

From the comparison result, it is easy to find that almost all of the results obtained are conservative, primarily at approximately 30%, and in some cases, even up to 50%. Although this can greatly guarantee the safety, it is inevitable to be too conservative in the design stage,

possibly resulting in great economic waste and loss with the popularization and application of frequency domain method. Alternatively, we know that the accuracy of the current frequency domain methods is not only related to the spectral type but also associated with the types of materials. However, it is quite important that the damage estimation method does not rely on the properties of material or PSD spectral type for real-life application. Thus, obtaining a new method with good universality and small relative error under the premise of safety is the problem to be further solved. Therefore, in this research, we attempt to find an optimal method in the sense that it can perform well, regardless of the test group being analysed. Furthermore, WL, TB2, DI, ZB, and SM methods, which perform relatively well, are chosen for a detailed analysis.

### 3 | PROPOSED NEW METHOD

#### 3.1 | The probability density distribution model

As mentioned in Section 1, the key step of the frequency method is to obtain the rain-flow amplitude and the rain-flow mean stress histogram (Figure 8) under random vibration and then determine the PDF.

Fatigue life is not only a function of stress amplitude but also a function of mean stress. Currently, several empirical formulas are proposed to account for the joint effect of stress amplitude and its mean on fatigue under constant amplitude loads, for example, Goodman equation. According to the response stress joint PDF and the Goodman equation, the fatigue damage can be determined:

$$D = \nu_p \int_{-\infty}^{\infty} \int_{s_{ae}}^{\infty} \frac{P(s_a, s_m)}{N_F} ds_a ds_m, \quad (28)$$

$$N_F = C \left( \frac{s_u s_a}{s_u - s_m} \right)^{-k}. \quad (29)$$

For harmonic stress processes, the amplitude and mean are known to be independent. For random stress processes, from the extensive simulations, it is can be found that the rain-flow amplitude and the rain-flow mean are weakly correlated.<sup>31,32</sup> We thus assume that they are independent<sup>33</sup> so that the joint PDF  $p(s_a, s_m)$  of these 2 variables can be expressed as

$$p(s_a, s_m) = p(s_a) \cdot p(s_m). \quad (30)$$

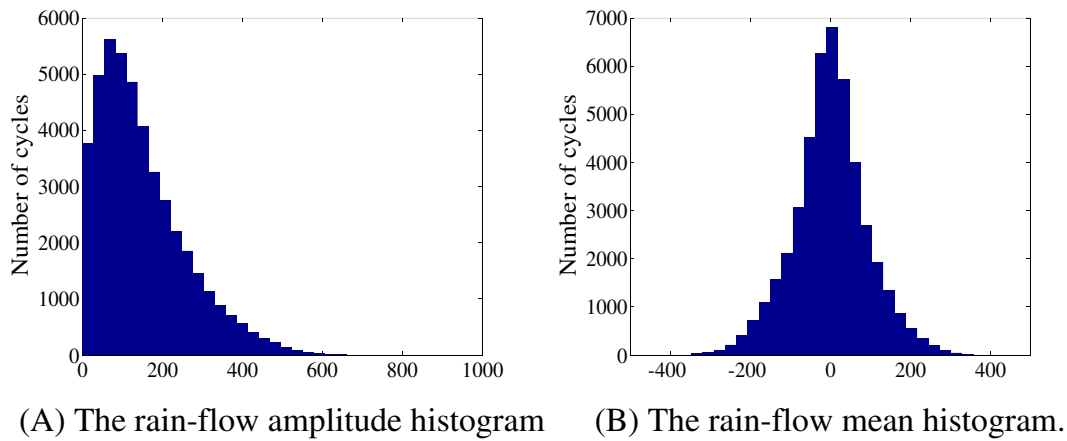


**FIGURE 8** The rain-flow amplitude and mean histograms. A, The rain-flow amplitude histogram and B, the rain-flow mean histogram [Colour figure can be viewed at [wileyonlinelibrary.com](http://wileyonlinelibrary.com)]

### 3.1.1 | Rain-flow amplitude PDF

As is known, the stress amplitude has a crucial effect on the fatigue life estimation, and the rain-flow amplitude PDF is the key step to estimate the random fatigue life by using the frequency method. A number of PDF empirical formulas have been developed for the frequency domain method; however, their estimates are too conservative. In this article, a new rain-flow amplitude PDF model with stronger stability and universality is proposed.

In practical engineering, the structural response under vibration load is commonly a wide-band random process, in which the band-limited white noise is one of the typical representatives. Thus, 57 groups of band-limited white noise spectra with spectral width parameter  $\varepsilon$  ranging from 0.1619 to 0.6661 were constructed to establish the rain-flow amplitude and mean PDFs model. After the time domain simulation and the rain-flow counting, the amplitude histogram can be obtained, as shown in Figure 8A. For fitting the probability density distribution, the Nakagami distribution is found to provide better agreement.

Nakagami probability density distribution<sup>34,35</sup> was first proposed in 1960; it has 2 parameters, the shape parameter  $m$  and the scale parameter  $\Omega$ , as given in the following expression:

$$p(s) = \frac{2m^m}{\Gamma(m)\Omega^m} s^{2m-1} \exp\left(-\frac{m}{\Omega} s^2\right). \quad (31)$$

In Figure 9A, the rain-flow amplitude histogram shows a long tail, which has a significant influence on the fatigue life estimation because the fatigue analysis involves high order moments of the rain-flow amplitudes. It is important to estimate the tail part of the PDF as accurately as possible. The existing PDF models generally use 1 or more of the Rayleigh distribution, the Weibull distribution, or their linear combinations; however, fitting the tail portion of the distribution accurately remains a problem. In most distribution functions, the decay rate of the Nakagami probability density distribution is the fastest one,<sup>36</sup> and the Nakagami probability density distribution can accurately estimate the

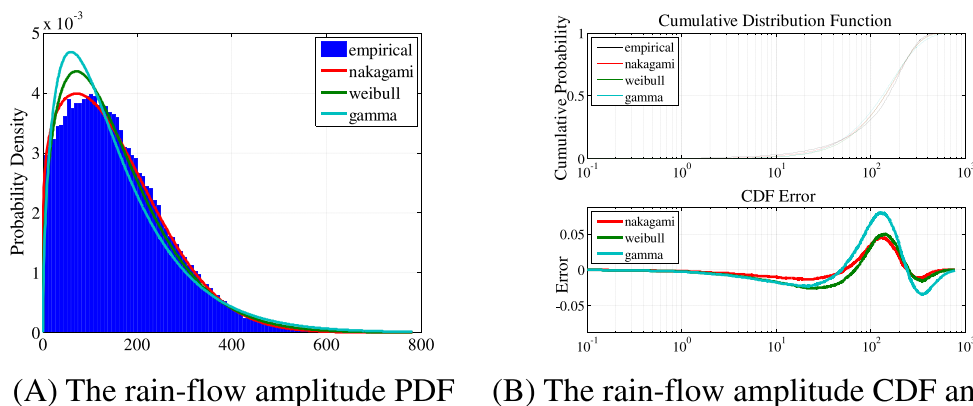


**FIGURE 9** The rain-flow amplitude. A, The rain-flow amplitude probability density function and B, the rain-flow amplitude cumulative distribution function (CDF) and error [Colour figure can be viewed at [wileyonlinelibrary.com](http://wileyonlinelibrary.com)]

probability density with a long tail in the high stress area. In addition, it has been found that, when the Nakagami distribution takes the shape parameter  $m$  values 1 and 1/2, the model can be transferred into a Rayleigh distribution and a single Gaussian distribution. When  $m > 1$ , the distribution is approximately equivalent to a Rice distribution.<sup>37</sup> The Nakagami distribution model not only captures the mode in the distribution but also gives a good approximation of the long tail.

To determine the 2 parameters of the Nakagami probability density distribution model, the parameters of the stress process affecting the fatigue analysis should be selected first. According to previous research studies, in this work, 2 main parameters should be considered: the standard deviation  $\sigma_x$  and the spectral width parameter  $\varepsilon$ . The spectral width parameter  $\varepsilon$  here is same as that in the Wirsching-Light method. By fitting 57 groups of band-limited white noise, the relationship between parameters  $m$ ,  $\Omega$  and the spectral moment  $\sigma_x$ ,  $\varepsilon$  are as follows:

$$\Omega = p_1 + p_2\sigma + p_3\sigma^2 + p_4\sigma^3 + p_5\sigma^4 + p_6\sigma^5 + \frac{p_7}{\varepsilon} + \frac{p_8}{\varepsilon^2} + \frac{p_9}{\varepsilon^3} + \frac{p_{10}}{\varepsilon^4}, \quad (32)$$

$$p_1 = -173484.44658; p_2 = 5430.95934; p_3 = -90.84265; p_4 = 0.75731; p_5 = -0.00302; p_6 = 4.65181\text{E-}6; p_7 = 60136.97954; p_8 = -23520.90118; p_9 = 3634.85426; p_{10} = -187.57862^\circ$$

$$m = q_1 + q_2 \ln(\sigma) + \frac{q_3}{\varepsilon} + \frac{q_4}{\varepsilon^2} + \frac{q_5}{\varepsilon^3} + \frac{q_6}{\varepsilon^4} + \frac{q_7}{\varepsilon^5}, \quad (33)$$

$$q_1 = -1.79861; q_2 = -0.11604; q_3 = 4.13812; q_4 = -2.16839; q_5 = 0.57314; q_6 = 0.07742; q_7 = 0.00423^\circ$$

The parameter fitting results can be shown in Figure 10:

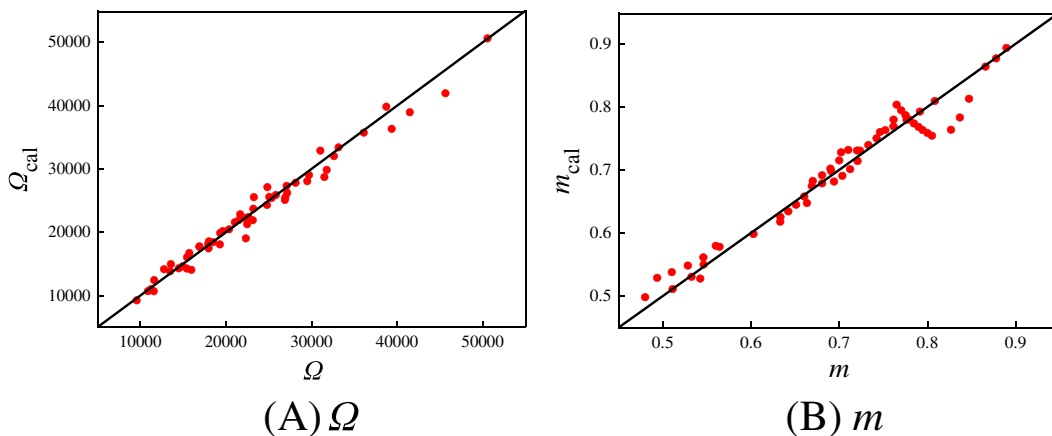


**FIGURE 10** Parameter fitting results. A,  $\Omega$  and B,  $m$  [Colour figure can be viewed at [wileyonlinelibrary.com](http://wileyonlinelibrary.com)]

### 3.1.2 | Rain-flow mean PDF

For a stationary Gaussian random process, most scholars believe that the rain-flow mean obeys a normal distribution and the mean stress is zero, with the mean histogram obtained shown in Figure 8B; thus, its impact on fatigue estimation can be ignored. To check this statement, the 57 groups of band-limited white noise were studied in the research. The rain-flow mean probability density distribution is found to be in good agreement with the  $t$ -location distribution, with the expected mean around zero, as shown in Figure 11.

The  $t$ -location distribution expression is as follows:

$$p(s) = \frac{\Gamma\left(\frac{\nu+1}{2}\right)}{\sigma\sqrt{\nu\pi}\Gamma\left(\frac{\nu}{2}\right)} \left(\frac{\nu + \left(\frac{s-\mu}{\sigma}\right)^2}{\nu}\right)^{-\frac{\nu+1}{2}}, \quad (34)$$

where  $\sigma$  is the scale parameter,  $\nu$  is the shape parameter, and  $\mu$  is the location parameter.

### 3.2 | Fatigue life estimation model

According to the rain-flow amplitude and the mean PDF, combined with the linear Miner cumulative rule and Equations 28 to 30, the fatigue damage is

$$\begin{aligned} D &= \nu_p \int_{-\infty}^{\infty} \int_{s_{ae}}^{\infty} \frac{p(s_a, s_m)}{C} \left(\frac{s_u s_a}{s_u - s_m}\right)^k ds_a ds \\ &= \nu_p \int_{s_{ae}}^{\infty} \int_{-\infty}^{\infty} \frac{p(s_a)}{C} s_a^k \cdot p(s_m) \left(\frac{s_u}{s_u - s_m}\right)^k ds_m ds_a \\ &= \nu_p \int_{s_{ae}}^{\infty} \frac{p(s_a)}{C} s_a^k ds_a \cdot \int_{-\infty}^{\infty} p(s_m) \left(\frac{s_u - s_m}{s_u}\right)^{-k} ds_m \\ &= \nu_p \int_{s_{ae}}^{\infty} \frac{p(s_a)}{C} s_a^k ds_a \cdot E \left(1 - \frac{s_m}{s_u}\right)^{-k}. \end{aligned} \quad (35)$$

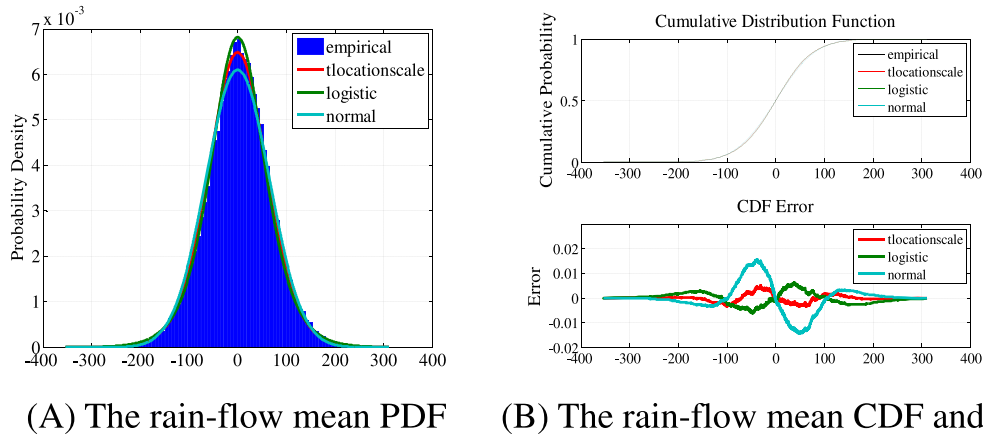


**FIGURE 11** The rain-flow mean. A, The rain-flow mean probability density function; and B, the rain-flow mean cumulative distribution function (CDF) and error [Colour figure can be viewed at [wileyonlinelibrary.com](http://wileyonlinelibrary.com)]

Assuming  $s_u \gg s_m$ , it can be simplified as follows<sup>38</sup>:

$$E\left(1 - \frac{s_m}{s_u}\right)^{-k} = 1 + \frac{k}{s_u}E(s_m) + \frac{k(k+1)}{2s_u^2}E(s_m^2). \quad (36)$$

According to Equation 34,  $s_m$  obeys the  $t$ -location distribution, and  $\mu = 0$ . Thus,

$$\begin{aligned} E(s_m) &= 0, \\ E(s_m^2) &= D(s_m) + [E(s_m)]^2, \\ E(s_m^2) &= D(s_m) = \frac{1}{\sigma^2 v - 2}, \\ E\left(1 - \frac{s_m}{s_u}\right)^{-k} &= 1 + \frac{k(k+1)}{2s_u^2} \frac{1}{\sigma^2 v - 2} \approx 1. \end{aligned} \quad (37)$$

Equation 36 can be simplified as

$$\begin{aligned} D &= \nu_p \int_{s_{ae}}^{\infty} \frac{p(s_a)}{C} s_a^k ds_a \cdot E\left(1 - \frac{s_m}{s_u}\right)^{-k} \\ &\approx \nu_p \int_{s_{ae}}^{\infty} \frac{p(s_a)}{C} s_a^k ds_a. \end{aligned} \quad (38)$$

Thus, for a Gaussian stationary random process, the rain-flow mean stress  $s_m$  obeys a  $t$ -location distribution, and  $E(s_m) = 0$ ; thus, the effect of the rain-flow mean stress can be ignored in the frequency domain fatigue life estimation, which can only consider the rain-flow amplitude.

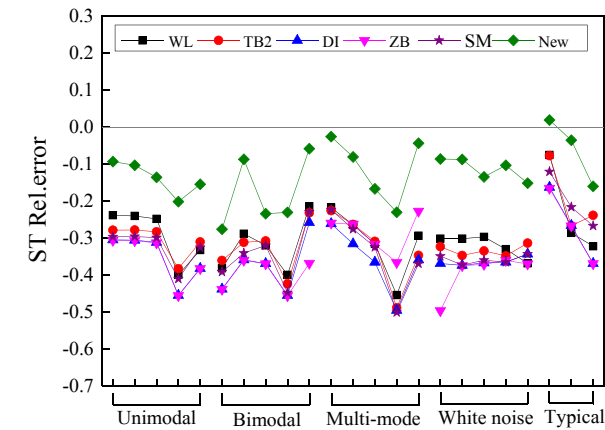
### 3.3 | Comparison and verification

An ideal frequency method for use in a design process should be consistent across different spectra and different slopes of the  $S$ - $N$  curve. The ideal method would give results that are close or equal to those given by a time

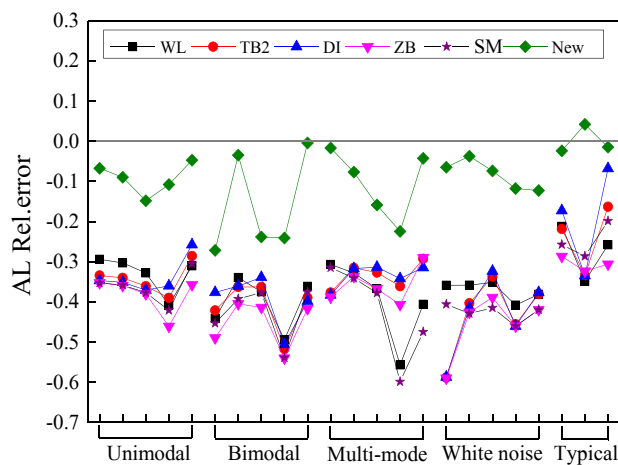
domain approach and preferably be conservative when not accurate. To verify the accuracy of the new method, comparisons between the new method and WL, TB2, DI, ZB, and SM methods according to analysis above in Tables 2, 3, and 4 were performed. The compared results are shown in Figure 12.

As shown in Figure 12, the results prove the conclusion again that, for traditional methods, the accuracy is not only related to the spectral type but also associated with the types of materials. The WL, TB2, and DI methods are in good agreement when the material fatigue parameter  $k$  is relatively low. With steeper slopes, the DI method is no longer applicable, whereas the WL and TB2 method are always valid. For typical engineering spectra, DI and TB2 provide better estimates; however, all the errors are high.

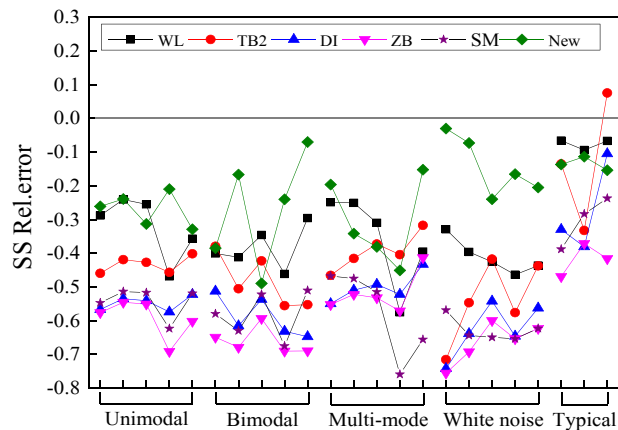
In contrast, the proposed method can effectively reduce the error. For the unimodal spectra, bimodal spectra, multimode spectra and white noise, the new method is well applicable for all the 3 types of material with smaller error compared with the WL, TB2, DI, ZB, and SM methods. Take the multimode spectra as an example. After comparison, the error of spectra with 3, 4, and 5 peaks are relatively stable; however, for 6 peaks, the chosen methods tend to underestimate the fatigue life. Similarly, TB2 and DI suit steel and aluminium well again, with only 20% to 40% error. However, at the highest value of the slope  $k$ , all the other methods fall behind WL in terms of accuracy. In contrast, the new method has a smaller error, with 20% for steel and aluminium, and between 20% and 50% for spring steel. The same conclusion was drawn for the typical engineering spectra. In the typical engineering spectra, DI and TB2 are highlighted as the best-performing methods, with the relative error of 10% to 30%; however, in some cases, TB2 appears slightly overestimated. The new method could



(A) Steel.



(B) Aluminum.



(C) Spring steel

**FIGURE 12** Comparison of relative errors. A, Steel; B, aluminium; and C, spring steel. Abbreviations: AL,  $\alpha_{0.75}$  method; DI, Dirlik method; SM, single-moment method; TB2, Tovo-Benasciutti method 2; WL, Wirsching-Light method; ZB, Zhao-Baker method [Colour figure can be viewed at [wileyonlinelibrary.com](http://wileyonlinelibrary.com)]

control the error within 20% for all the 3 materials; however, a slight overestimation of less than 5% is occasionally produced.

As verified through the above simulation spectra, the new method not only can be applied to different spectral type of PSD and different materials but also significantly decreases the error. Therefore, the new method can be used as a recommended frequency domain method for wide-band stationary Gaussian random-process fatigue life estimation in civil engineering and other fields.

## 4 | VERIFIED APPLICATION

Random vibration is widespread in many engineering structures in nature; such vibration causes the fatigue problems that cannot be ignored. In this section, the standard test specimen model (Figure 13A) of our previous study of the cast steel will be selected for the fatigue random vibration analysis.<sup>39</sup> The corresponding finite element model of the specimen is shown in Figure 13B, and the material type is cast steel G20Mn5QT (conditioning), which is a material commonly used in civil engineering.

### 4.1 | Modal and random vibration analysis

The intrinsic mode can be obtained by using the modal analysis method for the dynamic characteristics of the model. Through the calculation, the first-order self-oscillation frequency of vibration is 368.41 Hz, ie, the stiffness of the specimens is large, and the natural frequency is larger relative to the frequency of the engineering structure load; therefore, the basic resonance effect will not occur.

After the modal analysis, the incentive load spectrum, as shown in Figure 14, was applied by using ANSYS software. In this paper, the pressure PSD was applied to the standard specimen with the form of node incentives. Later, the stress solution of  $1\sigma$  and the response stress PSD of the maximum stress were calculated, as shown in Figure 15.

As Figure 15A shows, the maximum stress of  $1\sigma$  is 122.054 MPa. In 2 and 3  $\sigma$ , the maximum stresses are 244.108 MPa and 366.162 MPa, respectively. In addition, through the finite element calculation, the stress PSD of the maximum stress can be further obtained, as shown in Figure 15B.

### 4.2 | Random fatigue life estimation

The spectral moments and the parameter values of PDF are calculated from the stress power spectral density, as shown in Table 5.

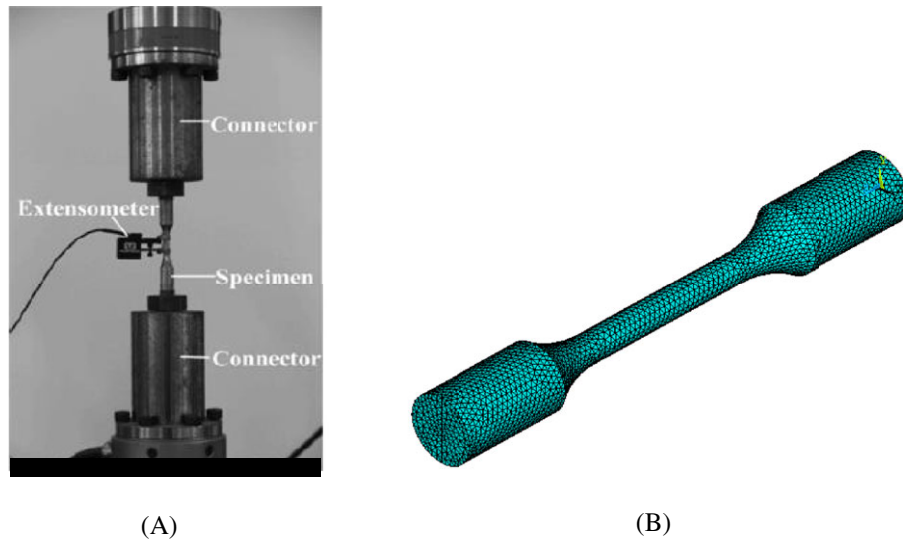


**FIGURE 13** Specimen model [Colour figure can be viewed at [wileyonlinelibrary.com](http://wileyonlinelibrary.com)]

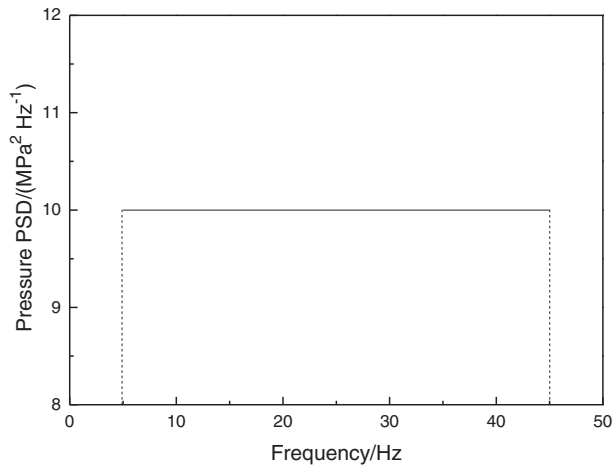


**FIGURE 14** Pressure load spectrum. PSD, power spectral density

Combining the PDF of stress amplitude described by various frequency domain methods and the Miner linear cumulative damage theory, the damage of the structure is

$$D = \sum D_i = \sum \frac{n_i}{N_i} \quad (39)$$

For the material of cast steel G20Mn5QT (conditioning), from the article,<sup>39</sup> the  $P$ - $S$ - $N$  curve with 50% survival probability is given as follows:

$$N = 1.9882 \times 10^{31} \times S^{-11.0132} \quad (40)$$

The simultaneous solution of Equations 39 and 40 can provide the fatigue damage of continuous distribution

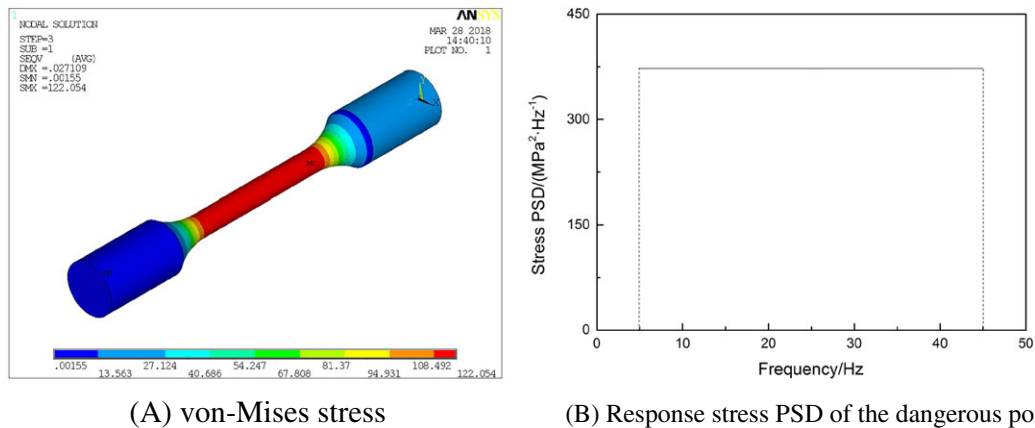


**FIGURE 15** Computed results. A, von-Mises stress and B, response stress power spectral density (PSD) of the dangerous point [Colour figure can be viewed at [wileyonlinelibrary.com](http://wileyonlinelibrary.com)]



**TABLE 5** Spectral moments and the parameter values of probability density function

$m_0$	$m_1$	$m_2$	$m_4$	$\alpha_{0.75}$
$1.4894 \times 10^4$	$3.7171 \times 10^5$	$1.1262 \times 10^7$	$1.3672 \times 10^{10}$	0.9396
$\alpha_1$	$\alpha_2$	$\varepsilon$	$\nu_0$	$\nu_p$
0.9076	0.7891	0.6142	27.4980	34.8384

stress state in the unit time via Equation 5 and provide the fatigue life of the structure via Equation 6.

Through the use of different frequency domain methods, the fatigue life of the structure can be obtained, in which the fatigue life estimation of the rain flow counting method (RF) is used as the control. The result of fatigue life by different methods is shown in Table 6.

From Table 6, it is reported that the results calculated by frequency domain methods, except the WL method and the proposed method, are too conservative compared with the time domain method for cast steel standard specimen, with errors exceeding 20%. The proposed frequency domain method in this paper has a smaller error and is safe, making it quite suitable for use. It can be verified that the new method can be used as a recommended frequency domain method for wide-band stationary Gaussian random-process fatigue life estimation in civil engineering and other fields.

### 4.3 | Comparison with constant fatigue

The pressure PSD should be transferred from the frequency domain to the time domain; the time history

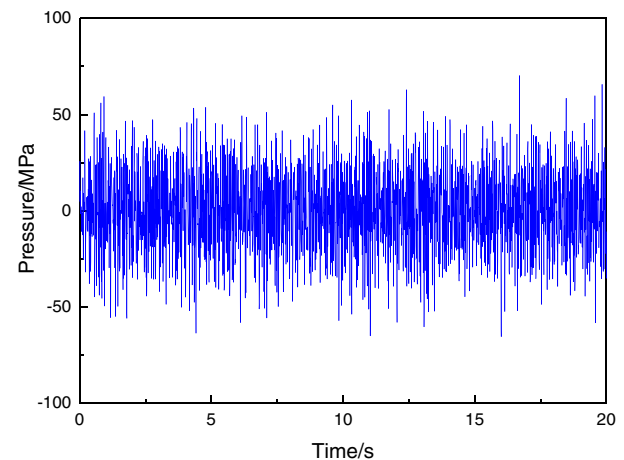
curve is shown in Figure 16. Because of the inverse Fourier transform, its random phase angle is not fixed, but uniformly distributed within the interval  $[0-2\pi]$ ; thus, 30 time domain samples for pressure PSD were simulated to reduce the accidental error. Each curve contains 4096 load amplitudes, in which the number of load amplitudes beyond 47.5 MPa range from 19 to 46, corresponding to approximately 0.46% to 1.12%. The 47.5 MPa here is equivalent to 273 MPa on the cast steel specimens in central; that is, the strain amplitude is 0.16%, and the test is in the state of  $R = -1$  in the references.

Because of the number of load amplitudes higher than 47.5 MPa is small, approximately 1%, the adverse effect on the fatigue life and beneficial effects caused by the high-load hysteresis effect of those loads can be ignored. Hence, all the stress amplitudes can be considered to be less than 47.5 MPa, which corresponds to the constant fatigue mentioned above. Because the load frequency is 10 Hz in the test, the fatigue life range under equivalent constant loading is approximately 5387 to 7200 seconds according to testing and calculations; these fatigue life values are greater than the fatigue life under random loading. Therefore, the fatigue life under the random load is lower than that under the constant load in the same situation. Random vibration analysis should be given more consideration in the design stage because such analysis is ignored frequently.

**TABLE 6** Comparison of fatigue life among estimation results

Method	Fatigue Life T/s	Relative Error
RF	1156	0
NB	573	50.43%
WL	1018	11.94%
AL	649	43.86%
OC	659	42.99%
TB1	573	50.43%
TB2	873	24.48%
DI	702	39.27%
ZB	653	43.51%
SM	704	39.10%
New method	971	16.00%

Abbreviations: AL,  $\alpha_{0.75}$  method ; DI, Dirlik method; NB, narrow-band method; OC, Ortiz and Chen method; SM, single-moment method; TB1, Tovo-Benasciutti method 1; TB2, Tovo-Benasciutti method 2; WL, Wirsching-Light method; ZB, Zhao-Baker method.

**FIGURE 16** Time history [Colour figure can be viewed at [wileyonlinelibrary.com](http://wileyonlinelibrary.com)]

## 5 | CONCLUSION

Fatigue problems are always a challenge for structures, and constant fatigue analysis is widely applied, in which the equivalent constant amplitude load instead of the actual variable amplitude load is adopted because of the uncertainty and complexity of the random load. A new frequency domain method for random fatigue life estimation in a wide-band stationary Gaussian random process was proposed in this research, and the results are summarized in detail as follows:

- A brief review and comparison were provided regarding existing frequency domain methods through the simulated PSD of different spectral types and different materials. The results showed that WL, TB2, and DI methods agree well for the material with small  $S-N$  curve slope  $k$  value. When  $k$  is large, WL and TB2 fit better. For typical engineering spectra, DI and TB2 are the most accurate. Therefore, TB2 is currently the best frequency domain method; however, it remains too conservative, with large error.
- A new frequency domain method was proposed. The new method could greatly reduce the error compared with the existing frequency domain methods and is well suited to the different types of PSDs and materials. Thus, the proposed method can serve as a recommended method in engineering applications.
- The rain-flow amplitude and mean PDF model for a wide-band stationary Gaussian random process were analysed, and the relationship with the statistical parameters of the PSD function was also established. For a wide-band stationary Gaussian random process that the expected mean of the rain-flow mean probability density distribution is around zero, the new fatigue life estimation model proposed considering the mean stress proved that one can ignore the effect of mean stress and only consider the rain-flow amplitude.
- A comparison between the random fatigue and the constant amplitude fatigue life was performed for the same cast steel G20Mn5QT model; the result showed the fatigue life under the random load is lower than that under the constant load. This observation is very interesting and useful because it indicates that the constant fatigue life estimation overestimated the antifatigue capacity of the real structures. From this point of view, random vibration analysis has a significant value.

## ACKNOWLEDGEMENTS

The authors acknowledge the support of National Natural Science Foundation of China (No. 51525803), National

Key Research and Development Plan of China under grant (2016YFC0701103) and Natural Science Foundation of Tianjin City (16JCQNJC07400).

## ORCID

Jie Xu  <http://orcid.org/0000-0002-6930-979X>

## REFERENCES

1. Peng C. *Fatigue Damage Research and Life Prediction of Prefabricated Cracked Concrete*. Wuhan, China: Wuhan University of Technology; 2013.
2. Shen W. *Fatigue Characteristics Research and Engineering Applications of the Non-Metallic Engineering Materials*. Dalian, China: Dalian University of Technology; 2013.
3. Gao Z, Moan T. Frequency-domain fatigue analysis of wide-band stationary Gaussian processes using a trimodal spectral formulation. *Int J Fatigue*. 2008;30(10-11):1944-1955.
4. Bishop NWM, Sherratt F. A theoretical solution for the estimation of "Rainflow" ranges from power spectral density data. *Fatigue Fract Eng Mater Struct*. 2010;13:311-326.
5. Lindgren G, Rychlik I. Rain flow cycle distributions for fatigue life prediction under Gaussian load processes. *Fatigue Fract Eng Mater Struct*. 2010;10:251-260.
6. Yeter B, Garbatov Y, Soares CG. Fatigue damage assessment of fixed offshore wind turbine tripod support structures. *Eng Struct*. 2015;101:518-528.
7. Park JB, Choung J, Kim KS. A new fatigue prediction model for marine structures subject to wide band stress process. *Ocean Eng*. 2014;76(1):144-151.
8. Park JB, Song CY. Fatigue damage model comparison with formulated tri-modal spectrum loadings under stationary Gaussian random processes. *Ocean Eng*. 2015;105:72-82.
9. Bendat JS, Piersol AG. Measurement and analysis of random data. *Technometrics*. 1966;10:869-871.
10. Qiang R, Hongyan W. Frequency domain fatigue assessment of vehicle component under random load spectrum. *J Phys: Conf Ser*. 2011;305:012060.
11. Wirsching PH, Light MC. Fatigue under wide band random stress. *J Struct Div*. 1980;106:1593-1607.
12. Chaudhury G. *Spectral Fatigue of Broad-Band Stress Spectrum with One or More Peaks*. Houston, Texas: Offshore Technology Conference; 1986.
13. Jiao G, Moan T. Probabilistic analysis of fatigue due to Gaussian load processes. *Prob Eng Mech*. 1990;5(90):76-83.
14. Benasciutti D, Tovo R. Spectral methods for lifetime prediction under wide-band stationary random processes. *Int J Fatigue*. 2005;27(8):867-877.
15. Dirlik T. *Application of Computers in Fatigue Analysis*. Warwick, USA: The University of Warwick; 1985.
16. Cianetti F, Alvino A, Bolognini A, Palmieri M, Braccetti C. The design of durability tests by fatigue damage spectrum approach. *Fatigue Fract Eng Mater Struct*. 2018;41(4):787-796.

17. Zhao W, Baker MJ. On the probability density function of rainflow stress range for stationary Gaussian processes. *Int J Fatigue*. 1992;14(2):121-135.
18. Han Q, Ye F, Xu J. Review of random fatigue research in civil engineering. *J Tianjin Univ*. 2016;49:143-151.
19. Petrucci G, Zuccarello B. Fatigue life prediction under wide band random loading. *Fatigue Fract Eng Mater Struct*. 2004;27(12):1183-1195.
20. Ortiz K, Chen NK. Fatigue damage prediction for stationary wideband processes, *Proc. Fifth Int. Conf. on Applications of Statistics and Probability in Soil and Struct. Engrg.*; 1987
21. Larsen CE, Irvine T. A review of spectral methods for variable amplitude fatigue prediction and new results. *Procedia Eng*. 2015;101:243-250.
22. Benasciutti D, Cristofori A, Tovo R. Analogies between spectral methods and multiaxial criteria in fatigue damage evaluation. *Prob Eng Mech*. 2013;31:39-45.
23. Quigley JP, Lee YL, Wang L. Review and assessment of frequency-based fatigue damage models. *SAE Int J Mater Manf*. 2016;9(3). <https://doi.org/10.4271/2016-01-0369>
24. Mršnik M, Slavič J, Boltežar M. Frequency-domain methods for a vibration-fatigue-life estimation—application to real data. *Int J Fatigue*. 2013;47(2):8-17.
25. Zuccarello B, Adragna NF. A novel frequency domain method for predicting fatigue crack growth under wide band random loading. *Int J Fatigue*. 2007;29(6):1065-1079.
26. Braccesi C, Cianetti F, Lori G, Pioli D. Fatigue behaviour analysis of mechanical components subject to random bimodal stress process: frequency domain approach. *Int J Fatigue*. 2005;27(4):335-345.
27. Halfpenny A. A frequency domain approach for fatigue life estimation from finite element analysis. *Key Eng Mat*. 1999;167-168:401-410.
28. Kihl DP, Sarkani S. Mean stress effects in fatigue of welded steel joints. *Prob Eng Mech*. 1999;14(1-2):97-104.
29. Tanegashima R, Ohara I, Akebono H, Kato M, Sugeta A. Cumulative fatigue damage evaluations on spot-welded joints using 590 MPa-class automobile steel. *Fatigue Fract Eng Mater Struct*. 2015;38(7):870-879.
30. Dong Q, Xu GN, Ren HL, Wang AH. Fatigue remaining life estimation for remanufacturing truck crane Jib structure based on random load spectrum. *Fatigue Fract Eng Mater Struct*. 2017;40(5):706-731.
31. Klemenc J, Fajdiga M. An improvement to the methods for estimating the statistical dependencies of the parameters of random load states. *Int J Fatigue*. 2004;26(2):141-154.
32. Xiangyu W. *Random Fatigue of Structures with Uncertain Parameters and Non-Gaussian Stress Response*. Delaware, America: University of Delaware; 2004.
33. Yi Y. *Vibration Fatigue Life Prediction Method Research Based On Stress Power Spectrum*. Hunan University, Hunan, China; 2014.
34. Nakagami M. The m-distribution—a general formula of intensity distribution of rapid fading. In: Hoffman WG, ed. *Statistical Methods in Radio Wave Propagation*. England: Pergamon, Oxford; 1960:3-6.
35. Zhou M, Zhang H, Peng Y. A simulation-based approach to estimate the correlation parameters of multivariate Nakagami-m distribution. *IEEE Commun Lett*. 2005;9(9):799-801.
36. Dersch U, Braun WR. A physical mobile radio channel model. *IEEE T Veh Technol*. 1991;40:472-482.
37. Surhone LM, Timplendon MT, Marseken SF. *Rice Distribution*. Hong Kong: Betascript Publishing; 2010.
38. Wang X, Sun JQ. On the fatigue analysis of non-Gaussian stress processes with asymmetric distribution. *J Vib Acoust*. 2005;127:1164-1166.
39. Han Q, Guo Q, Yin Y, Xing Y. Fatigue behaviour of G20Mn5QT cast steel and butt welds with Q345B steel. *Int J Steel Struct*. 2016;16(1):139-149.

**How to cite this article:** Han Q, Li J, Xu J, Ye F, Carpinteri A, Lacidogna G. A new frequency domain method for random fatigue life estimation in a wide-band stationary Gaussian random process. *Fatigue Fract Eng Mater Struct*. 2019;42: 97–113. <https://doi.org/10.1111/ffe.12875>